Metadata of the chapter that will be visualized online

Chapter Title	Convection-Enhanced Delivery in Children: Techniques and Applications	
Copyright Year	2022	
Copyright Holder	The Author(s), under exclusive license to Springer Nature Switzerland AG	
Corresponding Author	Family Name	**Aquilina**
	Particle	
	Given Name	**K.**
	Suffix	
	Division	Department of Neurosurgery
	Organization/University	Great Ormond Street Hospital
	Address	London, UK
	Email	Kristian.aquilina@gosh.nhs.uk
Author	Family Name	**Chakrapani**
	Particle	
	Given Name	**A.**
	Suffix	
	Division	Department of Metabolic Medicine
	Organization/University	Great Ormond Street Hospital
	Address	London, UK
	Email	Anupam.chakrapani@gosh.nhs.uk
Author	Family Name	**Carr**
	Particle	
	Given Name	**L.**
	Suffix	
	Division	Department of Neurology and Neurodisability
	Organization/University	Great Ormond Street Hospital
	Address	London, UK
	Email	Lucinda.carr@gosh.nhs.uk
Author	Family Name	**Kurian**
	Particle	
	Given Name	**M. A.**
	Suffix	
	Division	Department of Neurology and Neurodisability
	Organization/University	Great Ormond Street Hospital

	Address	London, UK
	Division	Neurogenetics Group, Developmental Neurosciences
	Organization/University	Zayed Centre for Research into Rare Disease in Children, UCL-Great Ormond Street Institute of Child Health
	Address	London, UK
	Email	Manju.kurian@ucl.ac.uk
Author	Family Name	**Hargrave**
	Particle	
	Given Name	**D.**
	Suffix	
	Division	Cancer Group
	Organization/University	UCL-Great Ormond Street Institute of Child Health
	Address	London, UK
	Email	d.hargrave@ucl.ac.uk

Abstract	Since its first description in 1994, convection-enhanced delivery (CED) has become a reliable method of administering drugs directly into the brain parenchyma. More predictable and effective than simple diffusion, CED bypasses the challenging boundary of the blood brain barrier, which has frustrated many attempts at delivering large molecules or polymers into the brain parenchyma. Although most of the clinical work with CED has been carried out on adults with incurable neoplasms, principally glioblastoma multiforme, an increasing number of studies have recognized its potential for paediatric applications, which now include treatment of currently incurable brain tumours such as diffuse intrinsic pontine glioma (DIPG), as well as metabolic and neurotransmitter diseases. The roadmap for the development of hardware and use of pharmacological agents in CED has been well-established, and some neurosurgical centres throughout the world have successfully undertaken clinical trials, admittedly mostly early phase, on the basis of in vitro, small animal and large animal pre-clinical foundations. However, the clinical efficacy of CED, although theoretically logical, has yet to be unequivocally demonstrated in a clinical trial; this applies particularly to neuro-oncology. This review aims to provide a broad description of the current knowledge of CED as applied to children. It reviews published studies of paediatric CED in the context of its wider history and developments and underlines the challenges related to the development of hardware, the selection of pharmacological agents, and gene therapy. It also reviews the difficulties related to the development of clinical trials involving CED and looks towards its potential disease-modifying opportunities in the future.

Chapter 6
Convection-Enhanced Delivery in Children: Techniques and Applications

K. Aquilina, A. Chakrapani, L. Carr, M. A. Kurian, and D. Hargrave

6.1 Introduction

Since it was first described in 1994, convection-enhanced delivery (CED) has undergone extensive pre-clinical and clinical investigations [1]. Although predominantly rooted in oncology, CED has been also used extensively in other fields in both adults and children, including neurodegenerative, metabolic, and neurotransmitter disorders. The unique ability of CED to reliably deliver macromolecules, nanoparticles, and viruses directly to their site of action in the brain, bypassing the blood brain barrier, continues to hold promise. In this article, we review the principles of CED and describe its techniques and applications in children.

K. Aquilina (✉)
Department of Neurosurgery, Great Ormond Street Hospital, London, UK
e-mail: Kristian.aquilina@gosh.nhs.uk

A. Chakrapani
Department of Metabolic Medicine, Great Ormond Street Hospital, London, UK
e-mail: Anupam.chakrapani@gosh.nhs.uk

L. Carr
Department of Neurology and Neurodisability, Great Ormond Street Hospital, London, UK
e-mail: Lucinda.carr@gosh.nhs.uk

M. A. Kurian
Department of Neurology and Neurodisability, Great Ormond Street Hospital, London, UK

Neurogenetics Group, Developmental Neurosciences, Zayed Centre for Research into Rare Disease in Children, UCL-Great Ormond Street Institute of Child Health, London, UK
e-mail: Manju.kurian@ucl.ac.uk

D. Hargrave
Cancer Group, UCL-Great Ormond Street Institute of Child Health, London, UK
e-mail: d.hargrave@ucl.ac.uk

6.2 The Blood Brain Barrier and Interstitial Fluid

The blood brain barrier (BBB) is the interface between the brain parenchyma and the vascular system. Its primary function is to maintain brain homeostasis by regulating transport into and out of brain cells. The architecture and development of the brain microvasculature is highly conserved across species. Early growth of brain capillaries has been extensively described in the zebrafish, where the development of BBB properties parallels early angiogenesis and is strikingly similar to the mammalian brain [2]. The human brain contains an extensive network of capillaries, with an average diameter of 7 μm, and an estimated surface area of 15–25 m². The vascular system of the brain is arranged such that each neuron is no further than 10–20 μm from the nearest capillary [3].

The BBB, at the level of the vascular endothelium, maintains homoeostasis for water, ions, amino acids, hormones, neurotransmitters, and immune cells as well as provides a barrier for toxic or infectious agents. In this way, it protects the brain against disruption of controlled neuronal signalling, inflammation, cerebral oedema, and exposure to pathogens. The neurovascular unit represents a structural and functional interaction between vascular cells (endothelial cells, pericytes), the basement membrane, and glial cells (microglia, astrocytes, and oligodendroglia). Endothelial cells are held together by interactions between the extracellular domains of transmembrane proteins, which are anchored on their intracellular side to the cytoskeleton. These prevent paracellular transport of molecules, enforcing the need for transcellular active transport. This is a dynamic interaction, such that increased shear stress due to blood flow upregulates genes associated with junctional proteins and transporters. Endothelial cells lack fenestrations and allow only low rates of transcytosis [4]. In the post-capillary venules, endothelial cells also have low expression of leucocyte adhesion molecules, allowing higher control of white cell recruitment to the perivascular spaces, limiting inflammation and oedema.

Brain capillaries are almost completely surrounded by astrocytic end feet. An astrocyte may support multiple endothelial cells. Astrocytes have a role in regulating blood flow in response to increased local neuronal activity, probably by changing calcium ion concentration in their end feet. The pericytes wrap around capillaries and are aligned with the direction of blood flow. They are separated from the endothelial cells by a thin 100 nm basement membrane. One pericyte typically supports three endothelial cells [5]. Pericytes are contractile, as they have actin fibres spread throughout their body; they can regulate capillary diameter and blood flow. They are recruited to nascent capillaries during development.

The extracellular space in the brain occupies 15–30% of the brain volume. It surrounds the neurons and glia in the brain and consists of a hyaluronan-based matrix and a fluid phase that contains lower protein, K^+, and Ca^{2+} concentrations than plasma but higher Mg^{2+} levels. Its fraction of total brain volume has been estimated at 0.15–0.30 [6]. The fluid phase represents a reservoir of ions and neurotransmitters and allows movement of solutes and nutrients between the most peripheral capillaries and the brain cells. It originates at the BBB, as the sodium–potassium pump

generates a net inflow of filtered plasma into the fluid phase [7]. CSF flow in the glymphatic system also mixes within the interstitial fluid, as it flows along the Virchow Robin spaces [8]. The geometry of the extracellular space has been described as an interconnected network of pores, up to 100 nm in diameter, running between adjacent cell membranes [6].

The BBB is a key obstacle in the treatment of several conditions that affect the CNS; only depression, schizophrenia, chronic pain, some of the white matter, neurotransmitter and autoimmune disorders, and epilepsy are currently treatable with orally administered small molecule drug therapy [3]. The BBB represents an important component of the gap between in vitro pharmacological success and patient outcomes in clinical trials. While small (<500 Da) lipophilic molecules can diffuse across the luminal and abluminal membranes of the endothelial cells, small polar molecules such as amino acids and nucleosides require carrier-mediated transport through the endothelial cells. Larger molecules such as proteins require endocytic transport, mediated by receptors or adsorption [3]. Efflux pumps actively return unwanted molecules back into the circulation. Ninety eight percent of all small molecules do not cross the BBB.

6.3 Convection-Enhanced Delivery: General Principles

6.3.1 Volume of Distribution

CED involves the bulk movement of a solute or drug along a pressure differential into the interstitial compartment, gradually replacing the extracellular fluid with infusate. The first injection studies, using blunt stainless steel 23G cannulae, were carried out in the corona radiata of anaesthetized cats, using a large (transferrin) and a small (sucrose) molecule [1]. These initial studies showed that 'microinfusion' could effectively raise the concentration of a substance within the brain parenchyma to several orders of magnitude of that in the systemic circulation. Early CED trials using diphtheria toxin for recurrent malignant gliomas demonstrated local tumour responses without systemic adverse effects [9].

CED was confirmed to be five to tenfold more effective than diffusion in delivering a substance [10]. Whereas diffusion is driven by a concentration gradient, CED can continue despite equal concentrations of the substance throughout the tissue. Distribution achieved by diffusion alone is limited to a maximum of 1–2 mm and is dependent on the size of the molecule. Diffusion is less effective for large molecules. There is a steep drop-off at the peripheral margin of the distribution, by about 250–1000-fold. In addition, the concentration of molecule at the point of dispersal must be very high, and therefore potentially toxic to brain tissue, at least at that point.

In contrast, CED, driven by a pressure differential, is able to distribute a molecule homogeneously throughout a high volume of interstitial brain tissue. Molecular size is not a limiting factor, as the interstitial fluid is displaced by bulk flow of the

solute containing the drug. Its eventual distribution is limited by the total volume infused, the metabolism of the drug, the degree to which it is bound to or taken up by the local cells, and whether it is transported back into the microvasculature. Distribution by CED is best for high molecular weight (>400 Da) hydrophilic molecules, which are therefore not easily cleared out of the interstitial fluid by absorption into the systemic circulation through the local capillaries. Large, hydrophilic molecules are more likely to remain in the interstitial fluid rather than diffuse back into the circulation [11]. Long infusion times allow a longer opportunity for metabolism and clearance at the periphery of the distribution cloud, leading to reduction in distribution volume [12]. As a continuous pressure differential is required, it is essential that the materials used to inject the drug into the brain, including the syringes, tubing, and implanted catheters, are made of stiff non-compliant materials.

Several variables affect delivery of the drug into the brain parenchyma. These include anatomy of the target site, infusion rate, infusion frequency, drug type and concentration, as well as catheter design and placement [11]. Delivery is defined by the ratio of the volume of brain permeated (V_d) by the volume infused (V_i). This varies by the permeability of the target brain tissue; a higher ratio implies superior delivery. Brain grey matter (cortex) has a lower interstitial fraction than white matter and has a typical distribution ratio of 4:1. White matter is more permeable and typically has a distribution ratio of 7:1. The high density of the white matter tracts in the brainstem gives it a typical ratio of up to 10:1. In addition, the anatomy of the target region defines the shape of permeation. In the cortex, flow is typically not constrained in any one direction (anisotropic) and fluid distribution is therefore spherical. In white matter, the direction of the tracts determines permeability, leading to isotropic distribution that is higher along the tracts.

The volume of distribution is also limited by ependymal and pial surfaces. Once the infused volume reaches these boundaries, the solute will then be lost to CSF. One study monitored the volume of distribution of gadoteridol-loaded liposomes infused by CED into non-human primates and canines [13]. This demonstrated that once leakage into the ventricles or sulci began, further distribution into the brain ceased or underwent marked attenuation. However, high molecular weight compounds may be contained by the pia and prevented from leaking into the subarachnoid space, if the pial surface itself is not punctured [14].

Particular issues related to the interstitial fluid and volume of distribution apply to CED in brain tumours. Brain tumours, especially higher-grade ones, disrupt the intercellular space and the physiological fluid flow within it. Neovascularization, increased permeability of immature blood vessels, sequestation of protein, and increased cellular components all raise fluid volume within the space and increase interstitial pressure [15]. The interstitial pressure in normal brain tissue is 0.8 mmHg, while within a tumour it has been measured at 7 mmHg [16]. Bulk flow of interstitial fluid from inside to outside the tumour may reduce the efficacy of CED. Cystic tumour components create their own local effects on the surrounding tumour tissue and brain parenchyma, depending on their content, fullness, and permeability, and the pressure within them may be different from that in the ventricles or subarachnoid space [17]. While in adult GBMs CED is usually administered after resection

of the tumour, this is not the case for diffuse intrinsic pontine glioma (DIPG) in children, where it is usually administered after radiotherapy. However, radiotherapy is known to degrade extracellular matrix, increasing its permeability [18]. Necrotic areas may act as sinks, reducing further forward flow of infusate. This is an important factor considering that in most current trials CED is administered after other treatment modalities have failed.

DIPGs can contain cystic regions; precise positioning of a catheter tip at least 10 mm from the cyst has been shown to preserve infusate volume, with avoidance of leakage into the cyst [19]. Regions of tumour necrosis lack interstitial architecture and may lead to pooling of the infusate, and highly vascular regions in malignant tumours can lead to infusate leaking into the systemic circulation [13]. The presence of a rich network of lenticulostriate vessels around the putamen may draw interstitial fluid and CED infusate into perivascular channels in a dorsoventral direction along a preferential extracellular flow pathway; a putaminal infusion approaching from a dorsal direction exploits this natural flow [20].

The volume of distribution is also influenced by viscosity and surface properties of the infused solute [21]. Monodispersed maghemite nanoparticles distributed better when their viscosity was increased by coating with dextran or when the infusate also contained sucrose or polyethylene glycol [22]. In a study evaluating delivery of viral particles, surface characteristics were found to be critical for their distribution [23]. Similarly, in another study evaluating spread of liposomes infused by CED, liposomes shielded by polyethylene glycol distributed further than unshielded liposomes [24]. Positively charged liposomes were also more effectively bound to cells, reducing their spread in comparison to neutral or negatively charged ones [24].

6.3.2   Infusate Backflow

High variability in flow rate and infusion patterns has made it harder to evaluate the impact of CED across clinical trials; infusion rates, for example, have ranged from 0.5 to 66 µL/min, and volumes infused from 2 to 108 mLs [11]. Infusions are usually commenced at a low rate, starting from 0.1 to 5 µL/min. The rate is slowly increased over subsequent hours. Effective infusion rates are specific to the catheter used and the target tissue. Historically, infusion rates have increased to enable sufficient drug delivery within a reasonable time. Although an increase in flow rate theoretically increases the volume of distribution, in practice this also leads to an increase in backflow along the cannula back towards the surface of the brain.

Backflow, or reflux, reduces pressure at the point of injection, limiting wide solute distribution. Once an annular gap around the catheter is formed, backflow is established, offering a path of least resistance and leading to loss of large volumes of fluid [25]. The needle tract effectively forms a pressure sink with lower hydraulic resistance than brain parenchyma [26]. Rotational movement during insertion may compromise the parenchymal seal around the cannula and increase reflux [27]. Conversely, rapid needle insertion may reduce parenchymal injury and reduce reflux

[28]. Reflux is more extensive, both in volume lost and distance travelled, when cannulas with large diameter are used [26]. When catheters similar to shunt catheters were used, either with a single opening at the end or with multiple side openings, distribution was poor; sealing of the burr holes, or use of a very low flow rate, was required to reduce large reflux [29, 30]. When multi-port hydrocephalus shunts were used, 80% of the fluid escaped through the three proximal holes, severely limiting any forward solute delivery [31]. The position of the catheter tip with regard to the tumour and peri-tumoural region, as well as distance from the ventricle, the cortical surface, and major sulcal boundaries, also influences the extent of backflow and success of solute delivery [14].

Backflow is also influenced by hydraulic resistance in the region of the ventricles. In computational three-dimensional models designed specifically to evaluate backflow and using realistic non-linear brain geometry, backflow varied with infusion flow rates, catheter distance from the ventricles, and intraventricular pressure [32]. Catheters implanted close to low-pressure ventricles were shown to lose more fluid to ventricular CSF, whereas catheters close to high-pressure ventricles had high backflow. The authors recognize that more accurate flow modeling must be patient-specific and needs to take into account heterogeneities of brain tissue, particularly in the vicinity of a tumour, and the changes in the mechanical properties of the parenchyma occurring as a result of cannula insertion and progressive infusion [32]. A recent study in adult rat brains has demonstrated the efficacy of electrokinetic CED of charged molecules along a current between two implanted electrodes; in this way, the infusion pressure, essential for CED, and the cause of backflow, is replaced by the electrophoretic mobility of the solute [33]. This technique also provides definitive directionality of distribution. Further pre-clinical studies are required to explore this concept further.

6.3.3 Catheters for CED

Catheters in current use are up to about 32G in diameter. Mechanical disruption and trauma of brain tissue around the catheter caused during insertion, as well as the presence of air bubbles, intermittent blockage, pressure spikes during infusion, large catheter diameter, and catheter hardness, all increase the volume and extent of backflow [34, 35]. Delaying the first injection to allow a longer tissue sealing time between the catheter and the brain has not been shown to effectively reduce backflow, probably because the healing time required is longer than the permissible waiting time. Insertion of a small soft catheter over a stylet increases the risk of introducing air bubbles. To limit this, catheters often have an outer coat that is more rigid, obviating the need for an internal stylet.

Five categories of catheter design have been described. These include the end-port cannula, stepped profile catheters, multi-port catheters, porous-tipped catheters, and balloon-tipped catheters [21]. Most have been evaluated in agarose gel phantoms, considered similar to brain tissue, although understandably more

homogenous and validated against the porcine brain model [36]. The microporous-tipped cannula is characterized by a ceramic tip containing a large number of small holes, up to 0.45 μm in diameter, arranged around the circumference of the catheter. As the holes are so small, pressure within the core distal to the proximal holes is maintained, allowing for a more even flow from the whole tip.

Porous catheters, with high porosity over a 13 mm segment, starting 4 mm from the tip, have been evaluated for infusion of large volumes of fluid over a wide distribution, such as an entire hemisphere [37]. When compared to the SmartFlow™ cannula, a step end-port catheter, used in vivo in porcine brain, larger distribution volumes were obtained with the porous catheter, as fluid emanated radially and uniformly from the entire porous length. Balloon-tipped catheters have been used only experimentally; these allow a small balloon at the top to be inflated within the post-resection tumour cavity, allowing the drug to be delivered into the periphery where tumour recurrence is most likely, without the risk of pooling or sequestration into the cavity [38]. The infusate was delivered effectively into the brain parenchyma around the balloon in a canine model to a depth of 25 mm, which would be expected to cover the region of recurrence in a glioblastoma [39]. In another study, the balloon did not have an exit port; it was filled with ^{125}I radiation source to deliver brachytherapy instead [40].

Stepped catheters have been used extensively for experimental and clinical CED and several designs have been developed. A step, fashioned close to the tip of the cannula, reduces reflux up the catheter, increases perfusion and interstitial pressure around the tip, and improves distribution (Fig. 6.1). The first stepped catheter was composed of a 0.2 mm needle with a glued-in silica tubing, 0.168 mm in external diameter, that extended beyond the tip of the needle by 5–10 mm [41]. Rigid cannulas, which contain ceramic or steel tubing with fused silica liners, are preferable for acute injection, as they minimize macro-motion during implantation and
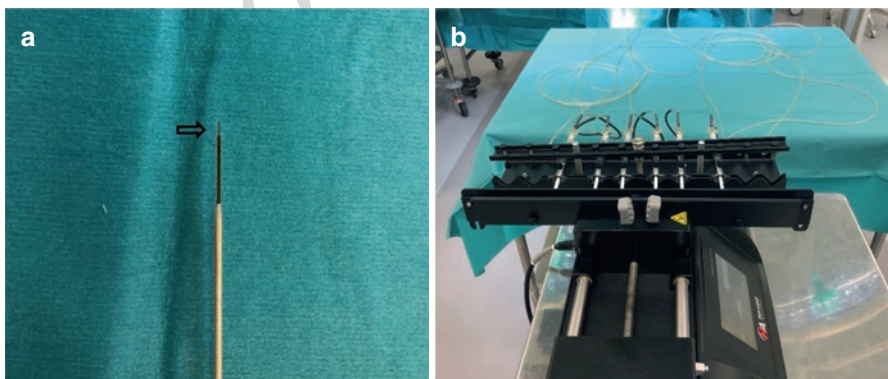

Fig. 6.1 (**a**) Tip of the Smartflow TM CED cannula. The block arrow points to the step proximal to the tip of the cannula, designed to prevent reflux. The body of the cannula is made of rigid ceramic. (**b**) Intraoperative infusion of AAV2 gene therapy for San Filippo syndrome, with six simultaneous infusions connected to the same Harvard syringe pump

injection [36]. For long-term implantation, however, the relative movement between the rigid cannula and the brain may promote reflux. A flexible cannula can move harmlessly with the frequent brain movements related to day-to-day activities. Subsequent developments included flexible cannulas with a rigid distal infusion tip, inserted over a removable rigid core. One of the first flexible catheter assemblies that was suitable for long-term implantation was used in a glial cell-line-derived neurotrophic factor (GDNF) study in Parkinson's disease [42].

Renishaw PLC have subsequently developed a recessed sub-millimetre diameter catheter in which two guide tubes, an inner and a longer outer one, form a step 1.5 mm long just proximal (3–18 mm) to the catheter tip; the inner guide tube is shorter than the outer one, thereby forming a recess which, on insertion, is plugged with tissue and therefore limits further reflux [25, 38]. The developers argue that this cannula does not act as a point source of distribution, but rather as a controlled reflux device [25]. A higher recess (or longer step length) led to a longer and narrower ellipsoid distribution; higher infusion flow rates led to reduced distribution. This applied to both in vitro and porcine grey matter evaluation (thalamic and putaminal) [25]. The authors argue that the distribution can be designed as spherical or ellipsoid by using catheters with shorter or longer recess length, aiming to match their target more completely. A step length between 3 and 6 mm causes a length to width ratio of 1:1–1:1.5 (spherical), whereas a step length over 12 mm increases the ratio to 2:1 or 3:1 (ellipsoid). Except for infusion at high pressures, the step limited further backflow around the cannula. Infusate rose to the step and then stabilized and distributed laterally. The highest reflux was seen with the shortest step lengths and the highest infusion rates. This study also showed that large backflow rates could be reduced by lowering infusion rates, but in vivo this would necessitate MR imaging during infusion [25]. These catheters are able to connect to a delivery system incorporating a transcutaneous port at the skull surface.

Another cannula involves a valve-tip device, where a solid rod is inserted into the core of the cannula, and on insertion, is withdrawn 3–5 mm. The design of the core is such that this allows infusate to flow around the rod, reducing the dead volume of the cannula [43].

Specialist pumps that are able to maintain such low flow rates are clearly required.

6.3.4 Catheter Insertion Techniques

Various aspects of catheter insertion procedures have been described in the recent literature. Implantation of the Renishaw stepped catheter utilizes image guidance and stereotactic robot assistance, based on the NeuroInspire software [25, 44]. Each component of the cannula is delivered over guide rods. The outer guide tube is delivered over a tungsten carbide delivery rod, just short of the implantation position. The inner guide tube is then passed over an inner steel rod under continuous aspiration to minimize entry of air into the tract. Finally, a 0.6 mm rod is advanced

beyond the inner guide tube to the injection point, creating a pre-formed track for the unsupported flexible cannula [25].

One of the principal difficulties in CED is the ability to visualize the distribution of the drug, ideally in real time, so that appropriate corrective action can be taken, if necessary, during the infusion to ensure complete coverage of the target. One technique to achieve real-time CED uses intraoperative MRI [45]. The ClearPoint navigation platform (MRI Interventions, Irvine, CA, USA) was developed to improve safety and accuracy of electrode implantation in deep brain stimulation and was subsequently modified to allow accurate drug delivery and real-time visualization in an intraoperative MRI setting [45, 46]. The SmartGrid, a localizing adhesive grid, is positioned over the expected entry site before MR volumetric scanning and informs the positioning of the SmartFrame, a scalp or skull-mounted frame which contains the infusion cannula guide. The ClearPoint software generates the trajectory and provides depth as well as co-ordinates on the XY axis. In addition, adjustments using hand controllers that extend beyond the bore of the magnet can be made by the neurosurgeon, allowing the expected error at the target to lie below 0.5 mm. A burr hole is then drilled through the mounted frame along the appropriate trajectory, and the SmartFlow cannula, after priming, is inserted to the required depth. Co-infusion with gadolinium allows real-time visualization of the injection; fast multiplanar T1 images are acquired every 5 min during the infusion. Once the infused fluid is seen in the target, the flow is increased as required by the protocol [45]. Bilaterally mounted SmartFrames allow simultaneous infusions in both hemispheres.

The aforementioned authors have used this system widely, including for the delivery of adeno-associated virus serotype 2 (AAV2), carrying a gene for amino acid decarboxylase (AADC), into the putamen of patients with medically refractory Parkinson's disease. The primary benefit of the technique is that the volume infused may be varied depending on the coverage of the putamen, as it is visualized in real time [45]. The system has also been used in early phase trials for recurrent glioblastoma, delivering nanoliposomal irinotecan and a retroviral replicating vector containing the gene for cytosine deaminase, an enzyme that converts the prodrug flucytosine to 5-fluorouracil in tumour cells. An implantable reservoir is currently being developed, opening the possibility of continuous long-term infusions.

A further development that has been trialled in non-human primate studies involves a frameless skull-mounted ball-joint guide array (BJGA) [27]. This device, made of PEEK and therefore MRI compatible, fixes to the skull through three screws; it rotates through 360° and has a maximum angulation of 16° to the vertical. Its centre contains three 2 mm holes, each allowing cannulas, electrodes, or biopsy needles up to 16 gauge to be inserted through. The device also contains fiducials filled with gadolinium that allows registration using T1-weighted MRI scans. The software allows the trajectory of the cannula to be matched to the pre-planned route. In a non-human primate study evaluating delivery along the long axis of the putamen, the mean Euclidean error at the target was 1.18 ± 0.60 mm. This is similar to the frame-based ClearPoint system, as evaluated in a small series of patients undergoing CED for DIPG or Parkinson's disease [47]; a significant contribution to this

336 error comes from non-linearities in the MR field. As in the ClearPoint system, real-
337 time visualization of the infusion is also possible [27]. The small size of the device
338 is particularly suited for paediatric use and allows multiple burr holes to be used
339 simultaneously, either bilaterally or unilaterally with multiple directions to the same
340 target. The three close parallel tracts allow real-time optimization of trajectory by
341 switching to an adjacent port as a 'rescue infusion'. Real-time adjustment in the
342 MRI scanner also allows compensation for brain shift, related to loss of CSF or
343 entry of air [27].

344   Matching distribution of infusate to the target remains a challenge, particularly
345 when the target is elongated or irregular and therefore difficult to cover with multi-
346 ple spherical infusion points. The 'infuse-as-you-go' technique has been described
347 in a study that infused AAV solution to the putamen of non-human primates through
348 an occipital trajectory [20]. The catheters were advanced in 2–4 mm increments
349 during the infusion, under real-time MR guidance. Coverage of the putamen was
350 superior to the standard transfrontal approach and could be achieved with a single
351 trajectory. No reflux along the infusion cannula was noted [20].

6.3.5 *Long-Term and Intermittent Infusions*

353 Delivery of chemotherapy to brain tumours using CED is unlikely to be effective if
354 only carried out once, or if general anaesthesia and insertion of a new catheter are
355 required for every injection episode. Maintenance of a stable volume of chemo-
356 therapeutic agent within the parenchyma allows the drug to target tumour cells over
357 various phases of the cell cycle. Prolonged use of external catheters connected to
358 intracranial CED cannulas is difficult due to the inherent infection risk. The typical
359 scenario in adults occurs after resection of the contrast-enhancing components of a
360 glioblastoma multiforme (GBM). Tumour cells are still likely to be present within
361 2–3 cm of the margins of the resection cavity. These cells, despite adjuvant therapy
362 with radiotherapy and temozolamide, are almost always the source of tumour recur-
363 rence. The ability to effectively infuse chemotherapeutic agents in this area, for a
364 prolonged period or at regular intervals, in a way that maintains a high dose through-
365 out the entire volume is required if CED is to be successful at prolonging survival.
366 In one phase 1b study, continuous 100 h infusions of topotecan, to a total infused
367 volume of 40 mLs, in 16 patients, in and around recurrent GBMs, using an external
368 catheter, demonstrated tumour regression in 69% of patients [48, 49]. GBM patients
369 in the cohort had a 20% 2 year survival, and one remains alive at submission of a
370 subsequent report in 2020 [50].

371   The proof of principle for prolonged CED was established in a study on adult
372 pigs [51]. A single catheter was implanted into the anterior limb of the right internal
373 capsule and connected to a Synchromed II pump (model 8637-20, Medtronic)
374 implanted subcutaneously. Topotecan was co-infused with gadolinium for 3 or
375 10 days. Maximum enhancement volume was reached by day 3 and remained stable
376 in those pigs that underwent 10 days of infusion [51]. The longer infusion period led

to a sustained volume of distribution beyond that achieved by the shorter 3-day infusion. Long-term topotecan infusion was well-tolerated in all animals.

A longer study by the same group has been published recently and describes important aspects of the effects of chronic infusions [12]. This involved infusion of topotecan in adult pig brains over periods ranging between 4 and 32 days. Infusions were carried out in the posterior centrum semiovale and were well-tolerated. A fully implantable system using a SmartFlow Flex ventricular catheter, 0.5 mm internal diameter (MRI Intervention Inc.), connected via a silastic lumbar catheter to a Synchromed II pump was used. The infusion pumps were emptied and refilled every 4–5 days. Typical infused volumes varied between 2 and 4 mLs per day. Priming the target tissue with a slow infusion for 1 or 2 days prior to increasing to a maximal dose reduced extravasation into the ventricles at the higher infusion rate. Drug distribution was measured by co-infusion with gadolinium. The distributed volume reached its peak early during the infusion and demonstrated a slight reduction as the steady state was reached [12]. Placement of the catheter tip within the sub-cortical white matter led to a distribution volume of 37.5% of the ipsilateral hemispheric volume; this was not significantly different between the short and long-term infusions, with most of the incremental gains in distribution occurring in the first 48 h, suggesting that a steady state equilibrium between infusion and clearance develops within 4 days of continuous infusion. This balance is dependent on local anatomy, and in this study, was significantly lower in the hippocampus. The maximal volume of distribution was achieved prior to the development of a steady state, suggesting that intermittent short-term dosing may still achieve the same levels of distribution. Despite the long-term infusion, none of the animals developed adverse effects, and no topotecan was detectable systemically.

The authors also conducted an in vitro study to demonstrate that the presence of gadolinium does not affect the cytotoxicity of topotecan on U87 human glioma cells. In addition, multiple biopsies taken prior to sacrifice demonstrated a significant positive correlation between gadolinium intensity and topotecan concentration. Histological analysis showed reactive astrocytes, microglia, and macrophages extending a few hundred microns from the catheter tip; this may be relevant to reducing backflow in long-term catheter implantation [12].

Another device that allows chronic or intermittent CED infusions has been developed by Renishaw PLC and has been used for recurrent glioblastoma, DIPG, and Parkinson's disease to infuse carboplatin, valproate, and GDNF [52–54]. The device consists of implantable catheters connected to a transcutaneous bone-anchored port [52]. In the first report on its use, a patient with recurrent glioblastoma underwent stereotactic implantation of four carbothane microcatheters, with an outside diameter of 0.6 mm, targeting the tumour enhancement and the peritumoural penumbra. The bone-anchored port was implanted using the skin-flap dermatome technique pioneered in bone-anchored hearing aid surgery. A dermatome was used to elevate a small flap of skin on an inferior pedicle, typically 25 mm in diameter; the underlying subcutaneous tissue was excised. The port was anchored to a burr hole in the skull bone at this site, the flap replaced, and the port then brought out through an opening in the skin flap. Infusions were begun on the third day, with

attachment of a needle administration device to the bone-anchored port. Hyperintensity on the T2-weighted MR sequence was used as a surrogate for volume distribution [52]. 12-h infusions were administered on three consecutive days, delivering a total volume of 27.9 mLs per day. Imaging showed a maximal distribution volume of 97.6 mLs, with a distribution to infusion ratio of around 3. Infusions were repeated using higher carboplatin concentrations at 4 weeks. Imaging at 8 weeks demonstrated an almost 50% reduction in the volume of contrast enhancement. Unfortunately, however, clear tumour progression was evident on further imaging 8 weeks later, outside the volumes of T2 signal change seen during the infusions. The patient subsequently died 8 months after implantation of the drug delivery system, and 33 months from diagnosis of her GBM [52]. All infusions were well-tolerated, with the exception of a single seizure on the third day of the first infusion set.

The ability to safely administer drugs by CED intermittently over long periods of time raises additional questions and opportunities. These include the development of infusion regimes to ensure satisfactory and efficient volume distribution, limit accumulation and toxicity, and allow periods of drug washout. Long-term scarring around catheter tips may modulate infusion volumes and require further development of catheter design and materials. For devices that use implanted pumps with an integral drug reservoir, the stability of the drug at body temperature needs to be addressed, as well as safe and easy ways of emptying and refilling the drug. The effects of long-term infusions on serial imaging also need further study.

6.4 Applications of CED in Paediatric Neuro-Oncology

Diffuse intrinsic pontine glioma (DIPG) remains the main tumour for which CED has been evaluated in children. DIPG carries the worst prognosis of all paediatric brain tumours. It typically presents between the ages of 5 and 10 years, with a classic triad of long tract signs, cranial neuropathies, and cerebellar signs [55]. Hydrocephalus, due to occlusion of the fourth ventricle related to tumour growth and infiltration in the fourth ventricular floor, is rare at presentation. Latency between symptom onset and diagnosis is almost always under 3 months [56]. Median survival following radiotherapy is around 10 months, with overall survival of 30% at 1 year, 10% at 2 years, and 1% at 5 years [57]. These statistics have not been improved for decades. Diagnosis is traditionally based on MR imaging, with a mass lesion that causes expansion of the pons, has poorly defined boundaries, occupies more than 50% of its axial diameter, remains clearly above the ponto-medullary junction, and often encircles the basilar artery. The lesion is hypointense on T1 and hyper-intense on T2-weighted imaging and may demonstrate variable enhancement with gadolinium. Contrast enhancement is an indicator of poor prognosis [58] (Fig. 6.2).

Stereotactic biopsy has been demonstrated to be safe, with diagnostic success of up to 96% and permanent morbidity of only 0.6% [59–61]. Biopsy has become
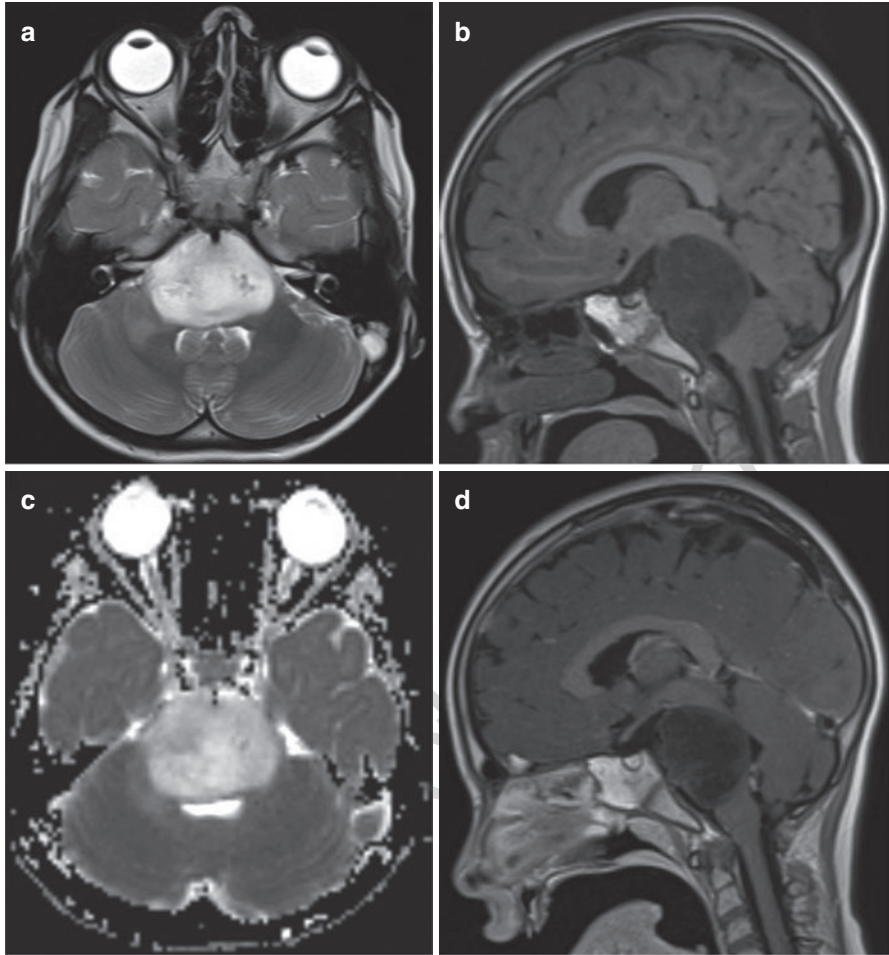
Fig. 6.2 Typical MR characteristics of DIPG, with large pontine mass, hyper-intense on T2-weighted axial image, encircling the basilar artery ventrally (**a**), and clearly delineated by the ponto-medullary junction on sagittal T1 sequence (**b**). The tumour does not restrict on diffusion-weighted imaging (**c**) and does not enhance on gadolinium administration (**d**)

more frequent as commitment to understanding the biology of DIPG and attempts to develop targeted therapy have intensified. Although routine biopsy has been advocated in several publications, a recent survey of European paediatric neurosurgeons suggested that most surgeons would only consider biopsy within the governance of a clinical trial [62, 63]. Biopsy specimens have consistently demonstrated the H3K27M mutation, and this has led to a revision of DIPG nomenclature in the WHO classification of CNS tumours as 'midline glioma, H3K27M mutant' [64]. Beyond these histone changes, several additional genomic aberrations emphasize the molecular diversity of this tumour [65].

In view of its infiltrative nature within the pons, cytoreductive surgery is not possible. Standard treatment involves focal, wide field radiation therapy to the pons, aiming to deliver up to 59.4 Gy in 30–33 fractions of 1.8 Gy daily [56]. Unfortunately, this is not curative, and the tumour recurs within months. Various chemotherapy regimens have been unsuccessful in improving the survival advantage conferred by radiotherapy alone. In particular, the use of concurrent temozolamide, effective in adult GBM, has had no impact on DIPG [66, 67]. Similarly, the addition of radiosensitizing agents such as topotecan, or raising the radiation dose to 78 Gy, has also had no impact on survival [68, 69]. The BIOMEDE trial offered targeted therapy with everolimus, erlotinib, or dasatinib based on biopsy findings; no statistical improvement in survival could be documented.

CED is a potentially promising drug delivery technique for DIPG. Unlike other high-grade tumours, which are usually associated with some degree of BBB compromise, DIPG appears to be protected by a relatively intact barrier, hence the frequent failure to enhance on MR imaging. Dosing of chemotherapeutic agents administered systemically is limited by toxicity. From a CED perspective, the factors for and against CED in DIPG have been clearly summarized by Tosi et al. [70]. The tumour is located within an anatomically defined region, and lack of previous surgery ensures that it has remained as homogeneous a tissue as possible prior to CED. Distant dissemination is not commonly seen on MRI early in DIPG. In addition, the uniformly poor prognosis, despite extensive research over at least two decades, may reduce the regulatory burden of new investigative techniques. On the other hand, the diseased brainstem in a young child is potentially vulnerable to stress and pressure, and the infusion of relatively large volumes of toxic substances may worsen its ability to function, with potentially dire neurological consequence [70].

Several pre-clinical and clinical studies have reported on the infusion of a number of drugs by CED into DIPG, including the radiolabelled monoclonal antibody Omburtamab, interleukin 13 pseudomonas toxin, panobinostat, small molecule kinase inhibitors, topotecan, and a combination of carboplatin and sodium valproate [30, 71–74] (Table 6.1). Panobinostat, a pan-histone deacetylase inhibitor, previously shown to have pre-clinical efficacy against DIPG, was evaluated in rat and porcine CED models and demonstrated satisfactory distribution without brainstem toxicity [73]. This is particularly encouraging considering that its ability to cross the blood brain barrier when administered intravenously is poor.

The highly complex nature of the brainstem, with its compact arrangement of long tracts and cranial nerve nuclei, may have been expected to preclude the infusion of high volumes of drug by CED. However, several studies have demonstrated relative safety of single, prolonged, and even multiple infusions [30, 71, 72, 75]. In the first reported CED of an agent into a DIPG, IL13-pseudomonas toxin, a chimeric fusion protein, was administered to a 4-year-old girl at recurrence [76]. The infusion was carried out through a single frontal catheter, using a co-infusion with gadolinium-DTPA, under direct MR imaging. A maximal infusion volume of 1.4 mLs was reached. A deterioration in the patient's sixth nerve palsy improved after 5 days of corticosteroid therapy. Although tumour progression was arrested by

Table 6.1 Clinical CED studies in DIPG in children, published to date

First author (Refs)	Publication date	Study	Number of patients	Agent	Trajectory	Catheter	Catheter placement	Duration and number of infusions
Lonser et al. [76]	2007	Single patient	1	IL-13 pseudomonas toxin	Frontal	Single, external	Stereotactic frame, MRI guidance	Single, continued to tumour coverage on iMRI
Anderson et al. [30]	2013	Pilot feasibility study	2	Topotecan	Cerebellar peduncles	Two, external	Stereotactic frame	100 h; single
Souweidane et al. [71]	2018	Dose escalation phase I	28	^{124}I-Omburtamab	Frontal	One, external	ClearPoint	1.18–15.53 h; single
Heiss et al. [72]	2019	Dose escalation phase I	5	IL-13 pseudomonas exotoxin	Frontal	One, external	Navigus Medtronic; ClearPoint	Up to 13 hours; one or two
Bander et al. [78]	2020	Dose escalation phase I	7	^{124}I-Omburtamab	Frontal	One, external	ClearPoint	One or two additional infusions (same as in ref)
Szychot et al. [75]	2021	Retrospective, compassionate use	13	Carboplatin and valproate	Frontal, cerebellar peduncles	Two, implanted	Renishaw, Neuroinspire	1–7 cycles, 3–6 weekly

4 weeks, the child died 4 months after treatment [76]. In another of the earlier studies, and the first to use the transcerebellar peduncle route, topotecan was delivered by CED through two catheters in two children with DIPG, following a tumour biopsy in the same procedure [30]. CED was continued for 100 h, but did not prolong survival in these two patients, and although low infusion rates were well-tolerated, high infusion rates up to 2.8 mLs/h resulted in new neurological deficits and deterioration in the KPS scores.

IL13-Psuedomonas toxin was also administered by CED to five children with DIPG through a single catheter in a single-institution phase 1 study [72]. Most glioma cell lines are known to overexpress IL13 receptors. In this study, it was hypothesized that Pseudomonas exotoxin is internalized by cells expressing IL13 receptors, which will lead to inhibition of protein synthesis and apoptotic cell death [77]. Complete tumour coverage was not obtained in any of the five patients. Two patients demonstrated short-term radiological benefit, with temporary arrest of disease progression. Two patients reported transient cranial nerve deficits and lethargy. Progression was radiologically evident by 12 weeks after infusion [72].

Outcomes of a first single centre phase 1 dose-escalation trial using CED of the radiolabelled monoclonal antibody Omburtamab were reported in 2018 [71]. This antibody was radiolabelled with ^{124}I; it targets the membrane-bound protein CD276 (B7-H3), which is overexpressed in DIPG and other paediatric brain tumours. Eligible patients were 3–21 years of age and had completed radiotherapy between 4 and 14 weeks before enrolment. In this way, changes in the tumour evaluated over a 30-day follow-up period were unlikely to be confounded by ongoing disease progression. Seven dose-escalation cohorts were planned, with the primary end point being the maximum tolerated dose. A semi-flexible catheter was inserted using the ClearPoint system, and ^{124}I—Omburtamab was infused in an intensive care environment. The prescribed dose ranged from 0.25 to 4.00 mCi, using an infused volume of 240–4540 μL at a rate of up to 7.5 μL/min [71]. The half-life of ^{124}I is 4.2 days, and therefore, as a true theranostic agent, is able to delineate drug distribution for several days, both in the brain and systemically, on PET imaging.

Twenty eight children were enrolled in this trial. No dose-related toxicity was observed, precluding the identification of the maximal tolerated dose. Only one patient developed treatment-related temporary hemiparesis. Estimated volumes of distribution were measured using MR and PET imaging and ranged from 1.5 to 20.1 cm^3, with a V_d to V_i ratio of 3.4. The distributions as measured on T2-weighted MRI and PET were not identical; distribution lasted for a longer period of time, up to a week, on PET imaging, and the V_d measured on PET was lower. The lesion to whole body ratio for the absorbed dose of radiation was higher than 1200. Although the authors emphasize that the purpose of the study was not to evaluate impact on survival, the median overall survival rate was 17.5 months, with 58.5% survival at 1 year and three patients surviving for more than 3 years [70, 71]. It is also important to note that at 30-day follow-up, 71% of the patients had performance indices identical to those at recruitment. In subsequent work, the authors have infused up to 8000 μL, obtaining volumes of distribution up to 35 mLs [70].

Seven of these children, who did not develop any evidence of tumour progression or toxicity within 30 days, went on to have further infusions of the same agent [78]. Six underwent a second infusion, and a seventh underwent a second and a third. Different entry sites and catheter trajectories were used. The distribution volume was not compromised on sequential infusions; in three patients where the new catheter tip was within 15 mm of the trajectory of a previous catheter, leakage of some of the infusate into an earlier track or injection site was noted. No significant adverse events were recorded.

A recent study has reported on a series of children who underwent CED with carboplatin and valproate for DIPG using a drug delivery system that allowed repeated infusion along four catheters [75]. All patients were treated on compassionate grounds after DIPG recurrence. Thirteen children were treated between 2017 and 2020. With the exception of two patients who developed persistent sixth nerve palsy, requiring reduction of drug concentration, all other adverse effects were transient. The four catheters, two frontal and two transcerebellar, were inserted stereotactically and positioned to optimize coverage of the pontine tumour, centrally and laterally. Infusion rates were started at 0.03 mL/h and increased incrementally to 0.3 mL/h. The side effect profile of each catheter was determined on the first infusion; the group developed the Pontine Infusion Neurological Evaluation (PIINE) score which defined the potential adverse effects of each catheter depending on its anatomical location [54]. Typically, infusions along the catheters were continued until the expected side effects occurred, at which point the infusion was discontinued. In this way, the maximal tolerated volume was infused every time. Infusions were repeated every 4–6 weeks. Infusion was commenced within 72 h of implantation. Infusions through three or four catheters simultaneously at rates of up to 3–5 µL/min were better tolerated than infusion through one or two catheters at higher flow rates. The estimated distribution was up to 30 cm^3 per day. Children were typically discharged within 24 h of finishing the infusion [75].

Baseline performance status was maintained in all patients up to the time of tumour progression. The median progression free survival was 13 months. The median overall survival was 15.3 months, with three out of the 13 patients alive and independently ambulant at the time of reporting. The last five patients received what the investigators considered as the optimal combination in terms of drug dosage and delivery; their median overall survival was 17.9 months at report [75]. This case series shows interesting preliminary activity which needs confirmation in a prospective clinical trial.

Several issues with regards to CED in DIPG are still unclear. None of the trials to date have advocated a biopsy in addition to CED. There is concern that a biopsy needle track may divert drug infused by CED and compromise optimal coverage of the tumour [79]. Frontal catheters are considered essential to ensure satisfactory tumour distribution and are positioned along a trajectory towards the long axis of a DIPG; they are therefore likely to interrupt the corticospinal tract. A study evaluating catheter position with corticospinal tractography, however, showed that catheter transgression of the tract and its incorporation in the volume of distribution only rarely resulted in a neurological deficit [80].

As DIPGs, like other infiltrative brain tumours, are already hyper-intense on T2-weighted MR imaging, the extent of tumour coverage during CED is difficult to determine. One case is described where ICOVIR-5, an oncolytic virus, was confused with Gd-DTPA [81]. This showed a satisfactory volume of distribution of the combined solute, which was completely washed out by 30 h. The authors emphasize that the duration of distribution is unrelated to the duration of the tumour's exposure to the virus, or indeed of any other drug, which is determined by the agent's specific cellular affinity, rather than by the continued association of the drug with Gd-DTPA [81]. In addition, as it is a relatively small molecule, Gd-DTPA may overestimate the distribution of a therapeutic agent [19].

The deformational changes in the brainstem caused by infusion of fluid into DIPG have been investigated [82]. This is particularly concerning, as the volume of distribution within the pons is greater than the volume of fluid infused, and any increase in pontine swelling can potentially worsen obstructive hydrocephalus or increase pressure on tracts and cranial nerve nuclei. Twenty three children with DIPG underwent volumetric evaluation of the pons and lateral ventricles pre-, 1 day post-, and 30 days post-infusion of a single dose of radioimmunotherapy. With a mean volume of infusion of 3.9 mLs, pontine volume increased by a mean of 2.5 mLs on day 1 post-infusion and tended to return to baseline by day 30. Lateral ventricle volume remained a mean of 5 mLs higher at 30 days compared to pre-infusion. None of the patients required a shunt within 90 days. The infusion volume had a weak positive correlation with the volume change in the pons and lateral ventricles, but changes in pontine volume did not relate to neurological deficits [82]. This study also suggests that an increase in pontine volume in the first month after CED is expected and not representative of tumour progression.

Oncological applications of CED in children are likely to extend beyond DIPG. Other tumours, such as thalamic, hypothalamic, and other midline high-grade gliomas (HGGs), as well as cortical ones, are sometimes not completely resectable. CED applied to unresectable components, either at recurrence or even at their primary presentation, may become a realistic option. Safety concerns and drug toxicity related to the eloquence of the brainstem may be less significant for tumours in these locations and therapeutic windows for supratentorial tumours may be wider. For example, pre-clinical evaluation of doxorubicin in mouse models of brainstem and thalamic HGG demonstrated that the maximum tolerated dose when infused to the thalamus was ten times that in the brainstem, allowing an effective dose to be reached in the thalamus but not in the brainstem [83].

CED has been evaluated extensively for adult HGGs and it is likely that some of these findings are translatable to some paediatric tumours. Glioblastoma multiforme (GBM) represents the commonest brain tumour in adults. Although there has been some progress over the last 10 years, its prognosis remains poor, with a median survival of up to 2 years [84]. Jahangiri et al. and Ung et al. have recently summarized some of the most relevant clinical and pre-clinical studies related to CED for GBM [49, 85]. Cytotoxins such as pseudomonas exotoxin targeted towards cell surface receptors that are overexpressed in glioma cells, such as the TGF-alpha, CD155, and IL4 receptors, have been used in phase I and II trials [86]. Topotecan,

gemcitabine, and carboplatin administered by CED to animal models showed better survival than controls [87, 88]. Bevacizumab administered by CED increased survival in an animal model over intravenous bevacizumab [89]. Fourteen clinical trials undertaken between 1997 and 2010 used conjugated toxins specifically taken up by glioma cells or chemotherapy agents that do not cross the BBB [85].

A notable improvement in a recent study was the inclusion of MRI-localized biopsies to allow study of the effects of drug infusion, in this case topotecan, on tumour cells and their microenvironment [50]. In addition, the importance of measuring neurocognitive function and quality of life after CED in recurrent HGG was underlined in a study on 16 patients who underwent single dose topotecan CED; most patients demonstrated stability on the Cognitive Stability Index and SF-36 over a 4 month follow-up period [90].

6.4.1 Reflections on CED Trial Failures in Oncology

CED should in theory be very effective treatment, yet the impact of CED in clinical trials has not been clear. Although these trials demonstrated the safety of CED, and many also showed some therapeutic efficacy, such as significant regression of recurrent GBM, overall success has been limited [48]. The translational model from animal to clinical studies, progressing from single to multiple to prolonged infusions, is well-illustrated by the long-term infusions of topotecan described above [49, 50].

One of the key issues related to trial failures in CED is catheter target accuracy and predictability of drug distribution, as shown in the phase III PRECISE trial, where IL 13-Pseudomonas exotoxin was delivered for recurrent GBM [91, 92, 93]. In this trial, fewer than half of the catheters had been optimally implanted, and although more accurate catheter placement correlated with a larger volume of distribution of agent, the coverage of the tumour was still low [92].

Another source of error, seen first in pre-clinical studies of gene therapy for Parkinson's disease, is the presence of perivascular spaces in the basal ganglia that divert the infusate away from the target [94]. Delivery platforms that allow real-time imaging, or the ability to change volumes in subsequent infusions, should mitigate against this problem.

Particularly in the context of chronic multiple infusions, it is essential that catheters are also placed in the periphery of a tumour, or where tumour recurrence may be expected. Attention to detail is required across a range of variables that also include the molecule, solute, and the histo-architecture of the target not just in the acute phase, but also in the longer term healing phase. This suggests that optimization of distribution needs to be tailored to the patient and to the catheter, as well as to the time from implantation, and the stage of the disease process. It is unlikely that a standard infusion regime will ever lead to an optimal distribution in all patients. For example, in a resection cavity, it has been shown that the catheter tips should be positioned 2 cm from the margin, in the direction of anticipated tumour progression [95]. Multiple catheters should be at least 2–4 cm apart and should avoid proximity

to the ventricle, subarachnoid space, and areas of necrosis or cystic degeneration [48].

The optimization of CED is a long translational process, which combines first principles and empirical pre-clinical, in vivo, and clinical evidence. Use of tracers is essential to allow optimization of coverage, and newer techniques using MR spectroscopy or PET imaging may be helpful.

Some mathematical models have been successful at predicting infusate distribution and coverage. These MRI-based models first identify fluid-filled cavities and surfaces, and using infusion volume, rate and catheter diameter calculate the extent of backflow and distribution with particular catheter positions [95]. The addition of diffusion tensor imaging has been useful [96]. More complex models have evaluated additional variables, including protein binding, cell uptake, and drug metabolism, as well as tissue permeability and drug diffusivity in different directions [97]. It is likely that a more refined understanding of the nature of interstitial fluid flow and bulk flow within the brain parenchyma, including that in the perivascular and perineuronal spaces, along white matter tracts, into the g lymphatics and along the meningeal layers is essential for optimization of CED [11].

Validation of the extent of drug distribution, at the correct dose, throughout the whole target volume is essential for a reliable assessment of outcome. Failure to cover the entire tumour leads to resistance and recurrence. In the study on CED of iodine-labelled omburtamab for DIPG, even in a small number of patients, the variance in tumour coverage was between 25 and 96% [71]. In addition, dosimetry considerations are site-specific. Pre-clinical studies have shown that agents such as doxorubicin are more likely to cause adverse effects when injected into the brainstem in DIPG animal models, rather than into the thalamus in similar HGG models; the dose tolerated in the thalamus was ten times higher [98].

The choice of drug is also relevant. A CED study using paclitaxel delivery to GBM was limited by toxicity [99]. Paclitaxel targets tubulin, stabilizing the microtubule polymer, in this way preventing cells from undergoing metaphase during mitosis. As microtubules are also required for nutrient transport in all cell types of the brain, paclitaxel delivered by CED also damages non-tumour cells. In contrast, topotecan, by binding to the DNA—topoisomerase complex, only affects dividing cells and is therefore expected to be safe and tumour-specific in the low replicative environment of the brain. Topotecan use for GBM has historically been limited by its poor BBB penetration and severe systemic side effects. Similarly, carboplatin, also used in CED, binds to DNA and inhibits successful replication.

The use of combined systemic treatment for tumours that may spread early beyond their local confines in the brain or brainstem is an important consideration. At the time of autopsy, up to a third of DIPG patients had leptomeningeal disease and a fourth had disease outside the brainstem [100]. However, this does not mean that local therapy such as CED is not useful. Focal radiotherapy has been the mainstay of treatment for DIPG for decades and is the only treatment modality that has improved survival. Focal surgical control, whenever possible, remains the first treatment to most brain tumours in adults and children. This suggests that the combination of a local with a systemic or CSF-delivered approach will need to be explored for DIPG.

6.4.2 New Trends and Opportunities in Neuro-Oncology

The combination of drugs with nanoparticle vehicles provides novel opportunities. Nanoparticles are typically 60–180 nm in size and have been investigated mostly in the context of GBM [101]. A size of about 70 nm appears to be ideal for delivery within the tumour interstitium [102]. Nanoparticles may promote drug retention in tissues, enhance accumulation of drug in specific regions, shield drugs from degradation processes, improve long-term and controlled release, and reduce toxicity to healthy tissue. Drugs that were previously deemed too toxic, insoluble, or chemically unstable may potentially be re-explored in combination with nanoparticles [101]. Successful delivery with nanoparticles may reduce the need for repeated or prolonged infusions. Liposomes, micelles, and polymeric nanoparticles have all been used in combination with CED [103].

Poly(lactic-*co*-glycolic acid) (PLGA) nanoparticles have been approved by the US Federal Drug Agency (FDA) and were used in a study evaluating its combination with carboplatin in rat and porcine CED models, as well as in glioma cell lines [104]. PLGA is biodegradable and breaks down into its natural metabolites lactic acid and glycolic acid. The study demonstrated that the combined drug provided greater tumour cytotoxicity and increased the tissue half-life of carboplatin. Similarly, PLGA combined with camptothecin and delivered by CED into rat models of high-grade glioma led to improved animal survival [105]. Camptothecin was present in tissues harvested 53 days after infusion, suggesting that this long tissue half-life may maintain exposure to the drug and potentially reduce the need for repeated dosing [105]. Nanoparticles may also support tumour imaging. 10 nm iron oxide nanoparticles conjugated to an antibody specific to the mutant epidermal growth factor receptor found on human GBM cells not only showed good efficacy against the tumour cells in vitro and in mouse models, but also allowed tumour cell and agent tracking by MRI [106].

Peptide-based nanofibres represent a new type of vehicle which are amenable to bind drugs and be infused by CED [102]. These carriers can be synthesized homogenously in various sizes, have a hydrophilic pegylated surface, and are, in addition, negatively charged, supporting more widespread parenchymal distribution. In a detailed evaluation, NFP-400 demonstrated the ideal size for wide convection, with a V_d to V_i ratio of 2.47, and reliably formed a sphere around the tip of the cannula; in terms of its clearance from the infused parenchyma, its half-life was calculated at 25 h. The larger NFP-1000 had a longer half-life, up to 42 h, but its large size meant that its distribution was poor, with a V_d to V_i ratio of 1.07. The smaller NFP-100 had a shorter half-life of about 18 h, but distributed effectively along white matter tracts, potentially making it the vehicle of choice for tumours infiltrating white matter such as DIPG [102].

Genetically modified T cells that express chimeric antigen receptors, CAR T cells, are now considered an important component of cancer immunotherapy and have shown remarkable success in the treatment of haematological malignancies. Radiological regression and increased survival have been demonstrated with CAR

782 T cells in GBM, and a number of trials are currently underway [107, 108]. In one
783 reported case involving a patient with diffuse recurrent GBM where the radiological
784 and clinical response persisted for 7.5 months after initiation of therapy, CAR T
785 cells were administered by direct intracavitary and intraventricular infusion using
786 separate catheters [107]. CAR T cells have also shown efficacy in mouse orthotopic
787 xenograft models of H3-K27M mutant paediatric diffuse midline gliomas [109]. In
788 an animal model of xenograft atypical teratoid rhabdoid tumour (ATRT), CAR T
789 cells delivered directly into the tumour and CSF showed significant benefits over
790 cells delivered intravenously, with higher potency at the tumour and lower levels of
791 peripheral inflammation [110]. However, the delivery of T cells by CED is challeng-
792 ing. Long delivery times inherent to CED lead to sedimentation of the T cells in
793 their saline medium. The use of a low viscosity hyaluronic acid-based hydrogel
794 carrier prevents sedimentation and allows homogenous delivery of T cells that
795 remain viable and active on deposition [111].

6.5 CED for Neurotransmitter Deficiency and Metabolic Disease

798 CED also provides an opportunity to deliver gene therapy to targeted cells within
799 the brain. Currently, gene delivery to the brain requires packaging of the DNA or
800 RNA within an AAV vector. This is a small non-replicative non-pathogenic virus
801 that lacks an envelope and adheres to the target cell membrane through heparin
802 sulphate proteoglycan receptors. It then undergoes endocytosis, with transport to
803 and release of the genetic material at the host nucleus. There it forms an extra-
804 chromosomal episome and enables the host cell to translate its nucleic acid on a
805 long-term basis. It can also integrate within the host genome at specific sites, as in
806 human chromosome 19. The absence of most viral proteins prevents an inflamma-
807 tory response to the virus. Although small, the 20 nm AAV does not penetrate the
808 BBB when administered intravenously. Pre-existing humoral immunity, thought to
809 be present in 32% of the population, may also prevent the virus from surviving in
810 the circulation [112]. When given through the CSF, it is unable to penetrate the
811 ependymal barrier. CED is therefore an effective way of transporting it to the brain
812 parenchyma [113].

813 Different viral capsids allow anterograde or retrograde transport along intercon-
814 nected circuits in a serotype-specific manner [113]. Transport to diffuse cortical
815 regions after CED to the thalamus in non-human primates has been explored [114].
816 Barua et al. were subsequently able to demonstrate in their swine model that CED
817 of AAV vectors into the white matter leads to specific and effective distribution into
818 the overlying cortex [115].

819 A number of trials using AAV vectors are currently underway and include stud-
820 ies on Parkinson's disease, mucopolysaccharidoses, AADC deficiency, and
821 Alzheimer's disease. In children, AAV2–AADC has been administered to

AADC-deficient patients. AADC is essential for the production of dopamine and serotonin from levodopa and 5-hydroxytryptophan, respectively. Children with AADC deficiency typically have a life expectancy of up to 7 years and present with movement disorders (hypotonia, hypokinesia, and dystonia), recurrent oculogyric crises, and autonomic dysfunction [116]. An early study involved infusion of AAV2–AADC into the putamen in ten children [117]. Although this did lead to an improvement in motor scores, the poor retrograde transport of AAV2 from the putamen to the substantia nigra and ventral tegmental pathways, where most of the dopamine is produced, compromised the benefits of this approach. A current trial is exploring the benefit of direct injection into the substania nigra and ventral tegmental areas and hopes to replicate the high AADC expression in the nigrostriatal and mesolimbic pathways which has been shown in non-human primate studies [118].

The mucopolysaccharidoses (MPS) are a group of rare monogenetic lysosomal storage disorders, caused by mutations in genes encoding proteins necessary for the breakdown of glycosaminoglycans. As a result, partially metabolized substrates accumulate in tissues, leading to widespread pathological effects that, in some, also include the central nervous system. MPS I (Hurler), II (Hunter) and IIIA and IIIB (San Filippo) involve the brain and are associated with progressive cognitive decline [119]. Bone marrow transplantation is effective at reducing only the systemic effects of MPS. Intravenous enzyme replacement does not cross the BBB and also has minimal effect on disease progression in the brain.

One of the earliest trials of CED in MPS was in Gaucher disease, due to glucocerebrosidase deficiency, where intravenous replacement of the enzyme had no effect on the neurological component of the disease [120]. CED into the frontal white matter in rats and subsequently in primates showed satisfactory activity of the enzyme in neurons throughout the infused frontal lobe and pons. This was subsequently replicated safely in a patient [121].

The MPS are considered ideal for gene therapy, as only one, known, gene is involved in a metabolic process that is well-understood and has been replicated in animal models. Lysosomal enzymes also transport well along axons and across synapses [122].

The injection of AAV vectors by CED has been investigated in MPS IIIA. In one trial, four MPS IIIA symptomatic patients, aged between 32 months and 6 years, underwent bilateral CED with an AAVrh10-based vector, using three hemispheric white matter trajectories on each side [123]. One-year data confirmed that the procedure and the vector were well-tolerated, with stabilization of brain atrophy on MRI in some patients. A larger phase II/III trial is currently underway.

6.6 Conclusion

The potential to deliver large molecules directly to target areas in the brain has developed enormously over the last 20 years. This has required collaboration across multiple disciplines, with most successful CED projects progressing through a

common pathway starting with identification of a promising agent, pre-clinical testing in small and large animals, and finally the multiple phases of a clinical trial to establish dosimetry, safety, and efficacy. Neurosurgeons have a unique practical understanding of the physiology and tolerance of the brain and have been intimately involved in this journey.

Further refinement of this process is necessary if clinical trials in CED are to become more successful, with continuous optimization of technology as well as prediction and visualization of volumes of distribution. A clear and well-defined roadmap, which could allow agents to be evaluated through a trusted delivery system, could accelerate the regulatory processes and ensure that successful agents can be made available to patients in a timely manner, particularly for diseases where no treatment currently exists, such as DIPG.

References

1. Bobo RH, Laske DW, Akbasak A, Morrison PF, Dedrick RL, Oldfield EH. Convection-enhanced delivery of macromolecules in the brain. Proc Natl Acad Sci U S A. 1994;91(6):2076–80.
2. Quiñonez-Silvero C, Hübner K, Herzog W. Development of the brain vasculature and the blood–brain barrier in zebrafish. Dev Biol. 2020;457(2):181–90.
3. Wong AD, Ye M, Levy AF, Rothstein JD, Bergles DE, Searson PC. The blood–brain barrier: an engineering perspective. Front Neuroeng. 2013;30(6):7.
4. Obermeier B, Daneman R, Ransohoff RM. Development, maintenance and disruption of the blood–brain barrier. Nat Med. 2013;19(12):1584–96.
5. Shepro D, Morel NM. Pericyte physiology. FASEB J. 1993;7(11):1031–8.
6. Syková E, Nicholson C. Diffusion in brain extracellular space. Physiol Rev. 2008;88(4):1277–340.
7. Abbott NJ. Evidence for bulk flow of brain interstitial fluid: significance for physiology and pathology. Neurochem Int. 2004;45(4):545–52.
8. Abbott NJ, Pizzo ME, Preston JE, Janigro D, Thorne RG. The role of brain barriers in fluid movement in the CNS: is there a "glymphatic" system? Acta Neuropathol. 2018;135(3):387–407.
9. Laske DW, Youle RJ, Oldfield EH. Tumor regression with regional distribution of the targeted toxin TF-CRM107 in patients with malignant brain tumors. Nat Med. 1997;3(12):1362–8.
10. Morrison PF, Laske DW, Bobo H, Oldfield EH, Dedrick RL. High-flow microinfusion: tissue penetration and pharmacodynamics. Am J Physiol. 1994;266(1 Pt 2):R292–305.
11. Stine CA, Munson JM. Convection-enhanced delivery: connection to and impact of interstitial fluid flow. Front Oncol. 2019;9:966.
12. D'Amico RS, Neira JA, Yun J, Alexiades NG, Banu M, Englander ZK, et al. Validation of an effective implantable pump-infusion system for chronic convection-enhanced delivery of intracerebral topotecan in a large animal model. J Neurosurg. 2019;133:1–10.
13. Varenika V, Dickinson P, Bringas J, LeCouteur R, Higgins R, Park J, et al. Detection of infusate leakage in the brain using real-time imaging of convection-enhanced delivery. J Neurosurg. 2008;109(5):874–80.
14. Sampson JH, Brady ML, Petry NA, Croteau D, Friedman AH, Friedman HS, et al. Intracerebral infusate distribution by convection-enhanced delivery in humans with malignant gliomas: descriptive effects of target anatomy and catheter positioning. Neurosurgery. 2007;60(2 Suppl 1):ONS89–98. discussion ONS98–9.

15. Soltani M, Chen P. Numerical modeling of interstitial fluid flow coupled with blood flow through a remodeled solid tumor microvascular network. PLoS One. 2013;8(6):e67025.
16. Boucher Y, Salehi H, Witwer B, Harsh GR, Jain RK. Interstitial fluid pressure in intracranial tumours in patients and in rodents. Br J Cancer. 1997;75(6):829–36.
17. Ali MJ, Navalitloha Y, Vavra MW, Kang EW-Y, Itskovich AC, Molnar P, et al. Isolation of drug delivery from drug effect: problems of optimizing drug delivery parameters. Neuro Oncol. 2006;8(2):109–18.
18. Leroi N, Lallemand F, Coucke P, Noel A, Martinive P. Impacts of ionizing radiation on the different compartments of the tumor microenvironment. Front Pharmacol. 2016;7:78.
19. Ivasyk I, Morgenstern PF, Wembacher-Schroeder E, Souweidane MM. Influence of an intra-tumoral cyst on drug distribution by convection-enhanced delivery: case report. J Neurosurg Pediatr. 2017;20(3):256–60.
20. Sudhakar V, Naidoo J, Samaranch L, Bringas JR, Lonser RR, Fiandaca MS, et al. Infuse-as-you-go convective delivery to enhance coverage of elongated brain targets: technical note. J Neurosurg. 2019;133:1–8.
21. Debinski W, Tatter SB. Convection-enhanced delivery for the treatment of brain tumors. Expert Rev Neurother. 2009;9(10):1519–27.
22. Perlstein B, Ram Z, Daniels D, Ocherashvilli A, Roth Y, Margel S, et al. Convection-enhanced delivery of maghemite nanoparticles: increased efficacy and MRI monitoring. Neuro Oncol. 2008;10(2):153–61.
23. Chen MY, Hoffer A, Morrison PF, Hamilton JF, Hughes J, Schlageter KS, et al. Surface properties, more than size, limiting convective distribution of virus-sized particles and viruses in the central nervous system. J Neurosurg. 2005;103(2):311–9.
24. MacKay JA, Deen DF, Szoka FC. Distribution in brain of liposomes after convection enhanced delivery; modulation by particle charge, particle diameter, and presence of steric coating. Brain Res. 2005;1035(2):139–53.
25. Lewis O, Woolley M, Johnson DE, Fletcher J, Fenech J, Pietrzyk MW, et al. Maximising coverage of brain structures using controlled reflux, convection-enhanced delivery and the recessed step catheter. J Neurosci Methods. 2018;1(308):337–45.
26. Chen MY, Lonser RR, Morrison PF, Governale LS, Oldfield EH. Variables affecting convection-enhanced delivery to the striatum: a systematic examination of rate of infusion, cannula size, infusate concentration, and tissue-cannula sealing time. J Neurosurg. 1999;90(2):315–20.
27. Sudhakar V, Mahmoodi A, Bringas JR, Naidoo J, Kells A, Samaranch L, et al. Development of a novel frameless skull-mounted ball-joint guide array for use in image-guided neurosurgery. J Neurosurg. 2019;132(2):595–604.
28. Casanova F, Carney PR, Sarntinoranont M. Influence of needle insertion speed on backflow for convection-enhanced delivery. J Biomech Eng. 2012;134(4):041006.
29. Tanner PG, Holtmannspötter M, Tonn J-C, Goldbrunner R. Effects of drug efflux on convection-enhanced paclitaxel delivery to malignant gliomas: technical note. Neurosurgery. 2007;61(4):E880–2. discussion E882.
30. Anderson RCE, Kennedy B, Yanes CL, Garvin J, Needle M, Canoll P, et al. Convection-enhanced delivery of Topotecan into diffuse intrinsic brainstem tumors in children. J Neurosurg Pediatr. 2013;11(3):289–95.
31. Lin J, Morris M, Olivero W, Boop F, Sanford RA. Computational and experimental study of proximal flow in ventricular catheters: technical note. J Neurosurg. 2003;99(2):426–31.
32. Orozco GA, Smith JH, García JJ. Three-dimensional nonlinear finite element model to estimate backflow during flow-controlled infusions into the brain. Proc Inst Mech Eng H. 2020;234(9):1018–28.
33. Faraji AH, Jaquins-Gerstl AS, Valenta AC, Ou Y, Weber SG. Electrokinetic convection-enhanced delivery of solutes to the brain. ACS Chem Nerosci. 2020;11(14):2085–93.
34. Mehta AM, Sonabend AM, Bruce JN. Convection-enhanced delivery. Neurotherapeutics. 2017;14(2):358–71.

35. White E, Bienemann A, Malone J, Megraw L, Bunnun C, Wyatt M, et al. An evaluation of the relationships between catheter design and tissue mechanics in achieving high-flow convection-enhanced delivery. J Neurosci Methods. 2011;199(1):87–97.

36. Chen Z-J, Gillies GT, Broaddus WC, Prabhu SS, Fillmore H, Mitchell RM, et al. A realistic brain tissue phantom for intraparenchymal infusion studies. J Neurosurg. 2004;101(2):314–22.

37. Brady ML, Raghavan R, Mata J, Wilson M, Wilson S, Odland RM, et al. Large-volume infusions into the brain: a comparative study of catheter designs. Stereotact Funct Neurosurg. 2018;96(3):135–41.

38. Lewis O, Woolley M, Johnson D, Rosser A, Barua NU, Bienemann AS, et al. Chronic, intermittent convection-enhanced delivery devices. J Neurosci Methods. 2015;259:47–56.

39. Olson JJ, Zhang Z, Dillehay D, Stubbs J. Assessment of a balloon-tipped catheter modified for intracerebral convection-enhanced delivery. J Neurooncol. 2008;89(2):159–68.

40. Tatter SB, Shaw EG, Rosenblum ML, Karvelis KC, Kleinberg L, Weingart J, et al. An inflatable balloon catheter and liquid ^{125}I radiation source (GliaSite radiation therapy system) for treatment of recurrent malignant glioma: multicenter safety and feasibility trial. J Neurosurg. 2003;99(2):297–303.

41. Fiandaca MS, Forsayeth JR, Dickinson PJ, Bankiewicz KS. Image-guided convection-enhanced delivery platform in the treatment of neurological diseases. Neurotherapeutics. 2008;5(1):123–7.

42. Gill SS, Patel NK, Hotton GR, O'Sullivan K, McCarter R, Bunnage M, et al. Direct brain infusion of glial cell line-derived neurotrophic factor in Parkinson disease. Nat Med. 2003;9(5):589–95.

43. Sillay K, Schomberg D, Hinchman A, Kumbier L, Ross C, Kubota K, et al. Benchmarking the ERG valve tip and MRI interventions smart flow neurocatheter convection-enhanced delivery system's performance in a gel model of the brain: employing infusion protocols proposed for gene therapy for Parkinson's disease. J Neural Eng. 2012;9(2):026009.

44. Barua NU, Lowis SP, Woolley M, O'Sullivan S, Harrison R, Gill SS. Robot-guided convection-enhanced delivery of carboplatin for advanced brainstem glioma. Acta Neurochir. 2013;155(8):1459–65.

45. Han SJ, Bankiewicz K, Butowski NA, Larson PS, Aghi MK. Interventional MRI-guided catheter placement and real time drug delivery to the central nervous system. Expert Rev Neurother. 2016;16(6):635–9.

46. Richardson RM, Kells AP, Martin AJ, Larson PS, Starr PA, Piferi PG, et al. Novel platform for MRI-guided convection-enhanced delivery of therapeutics: preclinical validation in non-human primate brain. Stereotact Funct Neurosurg. 2011;89(3):141–51.

47. Chittiboina P, Heiss JD, Lonser RR. Accuracy of direct magnetic resonance imaging-guided placement of drug infusion cannulae. J Neurosurg. 2015;122(5):1173–9.

48. Bruce JN, Fine RL, Canoll P, Yun J, Kennedy BC, Rosenfeld SS, et al. Regression of recurrent malignant gliomas with convection-enhanced delivery of topotecan. Neurosurgery. 2011;69(6):1272–9. discussion 1279–80.

49. Ung TH, Malone H, Canoll P, Bruce JN. Convection-enhanced delivery for glioblastoma: targeted delivery of antitumor therapeutics. CNS Oncol. 2015;4(4):225–34.

50. Upadhyayula PS, Spinazzi EF, Argenziano MG, Canoll P, Bruce JN. Convection enhanced delivery of topotecan for gliomas: a single-center experience. Pharmaceutics. 2020;13(1):39.

51. Sonabend AM, Stuart RM, Yun J, Yanagihara T, Mohajed H, Dashnaw S, et al. Prolonged intracerebral convection-enhanced delivery of topotecan with a subcutaneously implantable infusion pump. Neuro Oncol. 2011;13(8):886–93.

52. Barua NU, Hopkins K, Woolley M, O'Sullivan S, Harrison R, Edwards RJ, et al. A novel implantable catheter system with transcutaneous port for intermittent convection-enhanced delivery of carboplatin for recurrent glioblastoma. Drug Deliv. 2014;23(1):167–73.

53. Whone AL, Boca M, Luz M, Woolley M, Mooney L, Dharia S, et al. Extended treatment with glial cell line-derived neurotrophic factor in Parkinson's disease. J Parkinsons Dis. 2019;9(2):301–13.

54. Hollingworth MA, Zacharoulis S. Development of a clinical scale for assessment of patients with diffuse intrinsic pontine glioma (DIPG) receiving experimental therapy: the PONScore. J Neurooncol. 2020;149(2):263–72.

55. Hargrave D. Pediatric diffuse intrinsic pontine glioma: can optimism replace pessimism? CNS Oncol. 2012;1(2):137–48.

56. Clymer J, Kieran MW. The integration of biology into the treatment of diffuse intrinsic pontine glioma: a review of the North American clinical trial perspective. Front Oncol. 2018;8:169.

57. Grasso CS, Tang Y, Truffaux N, Berlow NE, Liu L, Debily M-A, et al. Functionally defined therapeutic targets in diffuse intrinsic pontine glioma. Nat Med. 2015;21(7):827.

58. Poussaint TY, Kocak M, Vajapeyam S, Packer RI, Robertson RL, Geyer R, et al. MRI as a central component of clinical trials analysis in brainstem glioma: a report from the pediatric brain tumor consortium (PBTC). Neuro Oncol. 2011;13(4):417–27.

59. Hamisch C, Kickingereder P, Fischer M, Simon T, Ruge MI. Update on the diagnostic value and safety of stereotactic biopsy for pediatric brainstem tumors: a systematic review and meta-analysis of 735 cases. J Neurosurg Pediatr. 2017;20(3):261–8.

60. Puget S, Beccaria K, Blauwblomme T, Roujeau T, James S, Grill J, et al. Biopsy in a series of 130 pediatric diffuse intrinsic pontine gliomas. Childs Nerv Syst. 2015;31(10):1773–80.

61. Grasso CS, Tang Y, Truffaux N, Berlow NE, Liu L, Debily M-A, et al. Functionally defined therapeutic targets in diffuse intrinsic pontine glioma. Nat Med. 2015;21(6):555–9.

62. Williams JR, Young CC, Vitanza NA, McGrath M, Feroze AH, Browd SR, et al. Progress in diffuse intrinsic pontine glioma: advocating for stereotactic biopsy in the standard of care. Neurosurg Focus. 2020;48(1):E4.

63. Tejada S, Aquilina K, Goodden J, Pettorini B, Mallucci C, van Veelen ML, et al. Biopsy in diffuse pontine gliomas: expert neurosurgeon opinion—a survey from the SIOPE brain tumor group. Childs Nerv Syst. 2020;36(4):705–11.

64. Louis DN, Perry A, Reifenberger G, Deimling von A, Figarella-Branger D, Cavenee WK, et al. The 2016 World Health Organization classification of tumors of the central nervous system: a summary. Acta Neuropathol. 2016;131(6):803–20.

65. Mackay A, Burford A, Carvalho D, Izquierdo E, Fazal-Salom J, Taylor KR, et al. Integrated molecular meta-analysis of 1000 pediatric high-grade and diffuse intrinsic pontine glioma. Cancer Cell. 2017;32(4):520–5.

66. Cohen KJ, Heideman RL, Zhou T, Holmes EJ, Lavey RS, Bouffet E, et al. Temozolomide in the treatment of children with newly diagnosed diffuse intrinsic pontine gliomas: a report from the Children's Oncology Group. Neuro Oncol. 2011;13(4):410–6.

67. Bailey S, Howman A, Wheatley K, Wherton D, Boota N, Pizer B, et al. Diffuse intrinsic pontine glioma treated with prolonged temozolomide and radiotherapy—results of a United Kingdom phase II trial (CNS 2007 04). Eur J Cancer. 2013;49(18):3856–62.

68. Packer RJ, Boyett JM, Zimmerman RA, Albright AL, Kaplan AM, Rorke LB, et al. Outcome of children with brain stem gliomas after treatment with 7800 cGy of hyperfractionated radiotherapy. A childrens cancer group phase I/II trial. Cancer. 1994;74(6):1827–34.

69. Chastagner VB, Grill J, Doz F, Bracard S. Topotecan as a radiosensitizer in the treatment of children with malignant diffuse brainstem gliomas. Cancer. 2005;104(12):2792–7.

70. Tosi U, Souweidane M. Convection enhanced delivery for diffuse intrinsic pontine glioma: review of a single institution experience. Pharmaceutics. 2020;12(7):660.

71. Souweidane MM, Kramer K, Pandit-Taskar N, Zhou Z, Haque S, Zanzonico P, et al. Convection-enhanced delivery for diffuse intrinsic pontine glioma: a single-centre, dose-escalation, phase 1 trial. Lancet Oncol. 2018;19(8):1040–50.

72. Heiss JD, Jamshidi A, Shah S, Martin S, Wolters PL, Argersinger DP, et al. Phase I trial of convection-enhanced delivery of IL13-pseudomonas toxin in children with diffuse intrinsic pontine glioma. J Neurosurg Pediatr. 2018;23(3):333–42.

73. Singleton WGB, Bienemann AS, Woolley M, Johnson D, Lewis O, Wyatt MJ, et al. The distribution, clearance, and brainstem toxicity of panobinostat administered by convection-enhanced delivery. J Neurosurg Pediatr. 2018;22(3):288–96.

74. Zhou Z, Ho SL, Singh R, Pisapia DJ, Souweidane MM. Toxicity evaluation of convection-enhanced delivery of small-molecule kinase inhibitors in naïve mouse brainstem. Childs Nerv Syst. 2015;31(4):557–62.

75. Szychot E, Walker D, Collins P, Hyare H, Shankar A, Bienemann A, et al. Clinical experience of convection-enhanced delivery (CED) of carboplatin and sodium valproate into the pons for the treatment of diffuse intrinsic pontine glioma (DIPG) in children and young adults after radiotherapy. Int J Clin Oncol. 2021;26(4):647–58.

76. Lonser RR, Warren KE, Butman JA, Quezado Z, Robison RA, Walbridge S, et al. Real-time image-guided direct convective perfusion of intrinsic brainstem lesions. J Neurosurg. 2007;107(1):190–7.

77. Kawakami M, Kawakami K, Puri RK. Interleukin-4-pseudomonas exotoxin chimeric fusion protein for malignant glioma therapy. J Neurooncol. 2003;65(1):15–25.

78. Bander ED, Ramos AD, Wembacher-Schroeder E, Ivasyk I, Thomson R, Morgenstern PF, et al. Repeat convection-enhanced delivery for diffuse intrinsic pontine glioma. J Neurosurg Pediatr. 2020;26(6):661–6.

79. Chittiboina P, Heiss JD, Warren KE, Lonser RR. Magnetic resonance imaging properties of convective delivery in diffuse intrinsic pontine gliomas. J Neurosurg Pediatr. 2014;13(3):276–82.

80. Morgenstern PF, Zhou Z, Wembacher-Schröder E, Cina V, Tsiouris AJ, Souweidane MM. Clinical tolerance of corticospinal tracts in convection-enhanced delivery to the brainstem. J Neurosurg. 2018;131(6):1812–8.

81. Tosi U, Souweidane MM. Longitudinal monitoring of Gd-DTPA following convection enhanced delivery in the brainstem. World Neurosurg. 2020;137:38–42.

82. Bander ED, Tizi K, Wembacher-Schroeder E, Thomson R, Donzelli M, Vasconcellos E, et al. Deformational changes after convection-enhanced delivery in the pediatric brainstem. Neurosurg Focus. 2020;48(1):E3.

83. Sewing ACP, Caretti V, Lagerweij T, Schellen P, Jansen MHA, van Vuurden DG, et al. Convection enhanced delivery of carmustine to the murine brainstem: a feasibility study. J Neurosci Methods. 2014;238:88–94.

84. Clark AJ, Lamborn KR, Butowski NA, Chang SM, Prados MD, Clarke JL, et al. Neurosurgical management and prognosis of patients with glioblastoma that progresses during bevacizumab treatment. Neurosurgery. 2012;70(2):361–70.

85. Jahangiri A, Chin AT, Flanigan PM, Chen R, Bankiewicz K, Aghi MK. Convection-enhanced delivery in glioblastoma: a review of preclinical and clinical studies. J Neurosurg. 2017;126(1):191–200.

86. Rand RW, Kreitman RJ, Patronas N, Varricchio F, Pastan I, Puri RK. Intratumoral administration of recombinant circularly permuted interleukin-4-pseudomonas exotoxin in patients with high-grade glioma. Clin Cancer Res. 2000;6(6):2157–65.

87. Degen JW, Walbridge S, Vortmeyer AO, Oldfield EH, Lonser RR. Safety and efficacy of convection-enhanced delivery of gemcitabine or carboplatin in a malignant glioma model in rats. J Neurosurg. 2003;99(5):893–8.

88. Kaiser MG, Parsa AT, Fine RL, Hall JS, Chakrabarti I, Bruce JN. Tissue distribution and antitumor activity of topotecan delivered by intracerebral clysis in a rat glioma model. Neurosurgery. 2000;47(6):1391–8. discussion 1398–9.

89. Wang W, Sivakumar W, Torres S, Jhaveri N, Vaikari VP, Gong A, et al. Effects of convection-enhanced delivery of bevacizumab on survival of glioma-bearing animals. Neurosurg Focus. 2015;38(3):E8.

90. Oberg JA, Dave AN, Bruce JN, Sands SA. Neurocognitive functioning and quality of life in patients with recurrent malignant gliomas treated on a phase Ib trial evaluating topotecan by convection-enhanced delivery. Neurooncol Pract. 2014;1(3):94–100.

91. Kunwar S, Chang S, Westphal M, Vogelbaum M, Sampson J, Barnett G, et al. Phase III randomized trial of CED of IL13-PE38QQR vs Gliadel wafers for recurrent glioblastoma. Neuro Oncol. 2010;12(8):871–81.

92. Mueller S, Polley M-Y, Lee B, Kunwar S, Pedain C, Wembacher-Schröder E, et al. Effect of imaging and catheter characteristics on clinical outcome for patients in the PRECISE study. J Neurooncol. 2011;101(2):267–77.

93. Sampson JH, Archer G, Pedain C, Wembacher-Schröder E, Westphal M, Kunwar S, et al. Poor drug distribution as a possible explanation for the results of the PRECISE trial. J Neurosurg. 2010;113(2):301–9.

94. Krauze MT, Saito R, Noble C, Bringas J, Forsayeth J, Mcknight TR, et al. Effects of the perivascular space on convection-enhanced delivery of liposomes in primate putamen. Exp Neurol. 2005;196(1):104–11.

95. Sampson JH, Raghavan R, Brady ML, Provenzale JM, Herndon JE, Croteau D, et al. Clinical utility of a patient-specific algorithm for simulating intracerebral drug infusions. Neuro Oncol. 2007;9(3):343–53.

96. Rosenbluth KH, Eschermann JF, Mittermeyer G, Thomson R, Mittermeyer S, Bankiewicz KS. Analysis of a simulation algorithm for direct brain drug delivery. Neuroimage. 2012;59(3):2423–9.

97. Zhan W, Rodriguez Y BF, Dini D. Effect of tissue permeability and drug diffusion anisotropy on convection-enhanced delivery. Drug Deliv. 2019;26(1):773–81.

98. Sewing ACP, Lagerweij T, van Vuurden DG, Meel MH, Veringa SJE, Carcaboso AM, et al. Preclinical evaluation of convection-enhanced delivery of liposomal doxorubicin to treat pediatric diffuse intrinsic pontine glioma and thalamic high-grade glioma. J Neurosurg Pediatr. 2017;19(5):518–30.

99. Lidar Z, Mardor Y, Jonas T, Pfeffer R, Faibel M, Nass D, et al. Convection-enhanced delivery of paclitaxel for the treatment of recurrent malignant glioma: a phase I/II clinical study. J Neurosurg. 2004;100(3):472–9.

100. Buczkowicz P, Bartels U, Bouffet E, Becher O, Hawkins C. Histopathological spectrum of paediatric diffuse intrinsic pontine glioma: diagnostic and therapeutic implications. Acta Neuropathol. 2014;128(4):573–81.

101. McCrorie P, Vasey CE, Smith SJ, Marlow M, Alexander C, Rahman R. Biomedical engineering approaches to enhance therapeutic delivery for malignant glioma. J Control Release. 2020;10(328):917–31.

102. Singh R, Bellat V, Wang M, Schweitzer ME, Wu YL, Tung C-H, et al. Volume of distribution and clearance of peptide-based nanofiber after convection-enhanced delivery. J Neurosurg. 2018;129(1):10–8.

103. Seo Y-E, Bu T, Saltzman WM. Nanomaterials for convection-enhanced delivery of agents to treat brain tumors. Curr Opin Biomed Eng. 2017;4:1–12.

104. Arshad A, Yang B, Bienemann AS, Barua NU, Wyatt MJ, Woolley M, et al. Convection-enhanced delivery of carboplatin PLGA nanoparticles for the treatment of glioblastoma. PLoS One. 2015;10(7):e0132266.

105. Sawyer AJ, Saucier-Sawyer JK, Booth CJ, Liu J, Patel T, Piepmeier JM, et al. Convection-enhanced delivery of camptothecin-loaded polymer nanoparticles for treatment of intracranial tumors. Drug Deliv Transl Res. 2011;1(1):34–42.

106. Hadjipanayis CG, Machaidze R, Kaluzova M, Wang L, Schuette AJ, Chen H, et al. EGFRvIII antibody-conjugated iron oxide nanoparticles for magnetic resonance imaging-guided convection-enhanced delivery and targeted therapy of glioblastoma. Cancer Res. 2010;70(15):6303–12.

107. Brown CE, Alizadeh D, Starr R, Weng L, Wagner JR, Naranjo A, et al. Regression of glioblastoma after chimeric antigen receptor T-cell therapy. N Engl J Med. 2016;375(26):2561–9.

108. Salinas RD, Durgin JS, O'Rourke DM. Potential of glioblastoma-targeted chimeric antigen receptor (CAR) T-cell therapy. CNS Drugs. 2020;34(2):127–45.

109. Mount CW, Majzner RG, Sundaresh S, Arnold EP, Kadapakkam M, Haile S, et al. Potent antitumor efficacy of anti-GD2 CAR T cells in H3-K27M+ diffuse midline gliomas. Nat Med. 2018;24(5):572–9.

110. Theruvath J, Sotillo E, Mount CW, Graef CM, Delaidelli A, Heitzeneder S, et al. Locoregionally administered B7-H3-targeted CAR T cells for treatment of atypical teratoid/ rhabdoid tumors. Nat Med. 2020;26(5):712–9.

111. Atik AF, Suryadevara CM, Schweller RM, West JL, Healy P, Herndon Ii JE, et al. Hyaluronic acid based low viscosity hydrogel as a novel carrier for convection enhanced delivery of CAR T cells. J Clin Neurosci. 2018;56:163–8.

112. Chirmule N, Propert K, Magosin S, Qian Y, Qian R, Wilson J. Immune responses to adenovirus and adeno-associated virus in humans. Gene Ther. 1999;6(9):1574–83.

113. Lonser RR, Akhter AS, Zabek M, Elder JB, Bankiewicz KS. Direct convective delivery of adeno-associated virus gene therapy for treatment of neurological disorders. J Neurosurg. 2020;134(6):1751–63.

114. Kells AP, Hadaczek P, Yin D, Bringas J, Varenika V, Forsayeth J, et al. Efficient gene therapy-based method for the delivery of therapeutics to primate cortex. Proc Natl Acad Sci U S A. 2009;106(7):2407–11.

115. Barua NU, Woolley M, Bienemann AS, Johnson D, Wyatt MJ, Irving C, et al. Convection-enhanced delivery of AAV2 in white matter—a novel method for gene delivery to cerebral cortex. J Neurosci Methods. 2013;220(1):1–8.

116. Brun L, Ngu LH, Keng WT, Ch'ng GS, Choy YS, Hwu WL, et al. Clinical and biochemical features of aromatic L-amino acid decarboxylase deficiency. Neurology. 2010;75(1):64–71.

117. Chien Y-H, Lee N-C, Tseng S-H, Tai C-H, Muramatsu S-I, Byrne BJ, et al. Efficacy and safety of AAV2 gene therapy in children with aromatic L-amino acid decarboxylase deficiency: an open-label, phase 1/2 trial. Lancet Child Adolesc Health. 2017;1(4):265–73.

118. San Sebastian W, Richardson RM, Kells AP, Lamarre C, Bringas J, Pivirotto P, et al. Safety and tolerability of magnetic resonance imaging-guided convection-enhanced delivery of AAV2-hAADC with a novel delivery platform in nonhuman primate striatum. Hum Gene Ther. 2012;23(2):210–7.

119. Hopwood JJ, Morris CP. The mucopolysaccharidoses. Diagnosis, molecular genetics and treatment. Mol Biol Med. 1990;7(5):381–404.

120. Lonser RR, Walbridge S, Murray GJ, Aizenberg MR, Vortmeyer AO, Aerts JMFG, et al. Convection perfusion of glucocerebrosidase for neuronopathic Gaucher's disease. Ann Neurol. 2005;57(4):542–8.

121. Lonser RR, Schiffman R, Robison RA, Butman JA, Quezado Z, Walker ML, et al. Image-guided, direct convective delivery of glucocerebrosidase for neuronopathic Gaucher disease. Neurology. 2007;68(4):254–61.

122. Lau AA, Hemsley KM. Adeno-associated viral gene therapy for mucopolysaccharidoses exhibiting neurodegeneration. J Mol Med. 2017;95(10):1043–52.

123. Tardieu M, Zerah M, Husson B, de Bournonville S, Deiva K, Adamsbaum C, et al. Intracerebral administration of adeno-associated viral vector serotype rh.10 carrying human SGSH and SUMF1 cDNAs in children with mucopolysaccharidosis type IIIA disease: results of a phase I/II trial. Hum Gene Ther. 2014;25(6):506–16.

Author Queries

Queries	Details Required	Author's Response
AU1	Please check and confirm if the affiliations are presented correctly.	
AU2	Please check the hierarchy of the section headings and confirm if correct.	